ASSESSING THERMAL RISK IN URBAN AREAS – AN APPLICATION FOR THE URBAN AGGLOMERATION OF ATHENS

Polydoros T. and Cartalis C.

Department of Environmental Physics, University of Athens, University Campus,
Build PHYS-V, Athens 15784
ckartali@phys.uoa.gr

Assessing thermal risk in urban areas is essential, as this can have major implications to human health and may influence quality of life in urban areas as well as the urban microclimate. Such assessment is promoted by estimating Land Surface Temperature (LST), evaluating the intensity of Surface Urban Heat Island (SUHI) and the variation of the discomfort index (DI), the latter reflecting the most common bioclimatic index used for outdoor thermal comfort applications. Calculations need to provide adequate spatial and temporal depictions of SUHI and DI, as these are correlated with such parameters as land cover/use, urban density, topography, etc. In this study an assessment of thermal risk in urban areas is made for the urban agglomeration of Athens in the event of summer heat waves.

Keywords: Thermal heat island, discomfort, urban environment and health

1. INTRODUCTION

It is usually observed that air temperatures in densely built-up urban areas are higher than the temperatures of the surrounding rural country. This phenomenon is known as ‘Urban Heat Island’ (UHI) and it has a significant impact on energy demand, human health and environmental conditions. The existence of the UHI is attributed to various causes: trapping of both incoming solar and outgoing longwave radiation, reduction of turbulent heat transport due to the geometry of the street canyons, decreased evapotranspiration and increased sensible heat storage due to construction materials, building and traffic heat losses as well as air pollution leading to increased long-wave radiation from the sky (Oke 1987).

The heat island phenomenon can be quantified by the maximum difference between urban temperature and the background rural temperature, which is defined as the urban heat island intensity (Oke, 1987). Heat island intensity depends on the size, population and industrial development of the city, the topography and the surface materials, the general climate of the region and the momentary meteorological conditions. In the study by Santamouris et al. (2001), it was found that during the summer period, daytime UHI intensity of Athens is close to 10°C for the central Athens area, whereas the night-time UHI intensity can rise up to 5°C.

Increased industrialization and urbanization in recent years have affected dramatically the number of urban buildings with major effects on the energy consumption of this sector. Urban areas without a high climatic quality use more energy for air conditioning in summer and even more electricity for lighting. Moreover, discomfort and inconvenience to the urban population due to high temperatures, wind tunnel effects in streets and unusual wind turbulence due to wrongly designed high rise buildings is a very common phenomenon (Santamouris et al., 2001).

Voogt and Oke (2003) review the use of thermal remote sensing for the study of urban climates with respect to the UHI effect and describe the distinction between the atmospheric UHI and the surface UHI. Atmospheric UHI is usually detected by ground-based air temperature measurements taken from standard meteorological stations, whereas surface UHI is observed from thermal remote sensors which record the upwelling thermal radiance emitted by the surface area that lies within the instantaneous field of view (IFOV) of the sensor. In contrast to atmospheric UHIs that are best expressed under calm and clear conditions at night, surface UHIs are usually studied by using satellite thermal remote sensing data of high spatial resolution (~ 100 m) acquired at daytime when heat island intensities are greatest (Roth et al., 1989).

Many surface UHI studies have been conducted using thermal remote sensing from satellites. These studies give a spatially continuous view of the surface UHI over large urban areas than is feasible using data from meteorological station networks. In addition, remote sensing can effectively depict the thermal environment of urban areas on a repeated basis. Thus, spatial coverage and temporal repetition are the main advantages of using satellite thermal remote sensing technique in the study of the urban climates (Stathopoulou et al., 2005)

The impact of the urban microclimate on the human thermal comfort is important. In urban environments, the commonly prevalent high temperatures, especially during the summer period, that produce the urban heat island effect, also tend to aggravate the comfort conditions of the city dwellers (Stathopoulou et al.,2005). Human discomfort can be evaluated through a number of theoretical and empirical biometeorological indices requiring usually a larger or smaller number of input parameters such as air temperature, wind speed, air humidity etc. The bioclimatic index most commonly used in urban climate studies to describe the level of thermal sensation that a person experiences due to the modified climatic conditions of an urban area is the Discomfort Index (DI) of Thom (Stathopoulou et al. 2005).

This paper explores the use of thermal Advanced Very High Resolution Radiometer (AVHRR) satellite data to map bioclimatic comfort conditions by estimating the Thom's discomfort index for the urban agglomeration of Athens in the event of summer heat waves for the period from 2008 to 2012.

2. METHODOLOGY AND DATA

The datasets used were acquired from the electronic library (CLASS) of the National Oceanic and Atmospheric Administration (NOAA).AVHRR data from NOAA-18 and NOAA-19 satellites were selected for daytime because the satellites time of overpass is near noon time when the highest daily air temperatures occur. For nighttime, AVHRR data from MetOp-A satellite were selected as the overpass time is around 22.30 local time (19.30 UTC).

2.1 AVHRR data processing

AVHRR thermal images (spatial resolution at 1.1 km) were used in order to map the thermal urban environment of the city of Athens. Images were geometrically and radiometrically corrected; radiometric calibration of the images involved the conversion of the raw digital number (*DN*) values to spectral radiance and then to at-sensor reflectances for the visible channels 1 (0.58-0.68μm) and 2 (0.725 1.10μm) and to brightness temperatures for the thermal channels 4 (10.3-11.3μm) and 5 (11.5-12.5μm). The conversion to brightness temperatures from spectral radiances was performed using the inversion of Planck's blackbody equation. Next a cloud mask was applied to all images in order to ascertain their correspondence to clear sky conditions. For daytime images all pixels with channel 1 reflectance greater than 25% were considered as cloud contaminated and were rejected. For nighttime images an algorithm for cloud detection (Saunders and Kriebel, 1988) was used. The algorithm is based on channel 3, 4 and 5 temperature values as well as on the temperature differences of T4-T5 and T3-T4. Finally all images were geo-referenced to the Geographic (Lat/Lon) map projection system (Spheroid: WGS 84, Datum: WGS 84).

2.2 Urban Atlas data processing

The Urban Atlas dataset was used in order to identify the urban, suburban and rural regions of the greater Athens area. For this purpose, the initial 20 classes were merged into only three classes defined as Urban, Suburban and Rural Areas. The aggregate land cover type allows the spatial discrimination between the different urban land covers that are related to the SUHI phenomenon and also favors the spatially accurate assignment of the surface emissivity that corresponds to these urban land covers.

2.3 Land surface temperature (LST)

The algorithm selected for this study for the estimation of LST using AVHRR thermal infrared data was developed by Coll et al. (1994a). It requires the brightness temperatures in AVHRR channels 4 and 5, the mean emissivities and the spectral emissivity difference in these channels. It also uses coefficients which depend on atmospheric moisture and the surface temperature. These coefficients can be optimized according to the characteristics of a given area. The algorithm is described by the relation:

$$LST = T4 + [1 + 0.58\cdot(T4 - T5)]\cdot(T4 - T5) + 0.51 + \alpha\cdot(1 - E) - \beta\cdot(\Delta\varepsilon)$$

where:

T4 is the radiance temperature for channel 4 of AVHRR,
T5 is the radiance temperature for channel 5 of AVHRR,
E is the mean spectral emission coefficient for channels 4 and 5:

$$E = (\varepsilon4 + \varepsilon5)/2$$

where:

$\varepsilon 4$ is the surface emission coefficient for channel 4,
$\varepsilon 5$ is the surface emission coefficient for channel 5,
and $\Delta\varepsilon$ is the difference of the emission coefficients for channels 4 and 5:

Values for E and $\Delta\varepsilon$ were taken from Stathopoulou et al (2004) and are shown in Table 1. Coefficients α and β in equation (1) depend on the amount of atmospheric water vapour in the area of the satellite image and from the temperature of the surface under observation. They may be described as a function of the brightness temperature (T4) which is recorded in channel 4 of the AVHRR and the precipitable water (PW) in the area (Caselles et al. 1997).

$$\alpha = (0{,}190 \cdot PW - 0.103) \cdot T4 - 67 \cdot PW + 107$$

$$\beta = (0{,}100 \cdot PW + 1{,}118) \cdot T4 - 68 \cdot PW - 163$$

where PW is in gr/cm2 and T4 in °K. Monthly mean PW values for the region of Greece from Chrysoulakis and Cartalis (2002) were used in this study.

Table 1: Emisivity values by land cover type.

Land cover type	Mean emissivity	Emissivity difference
Urban	0.97	-0.007
Suburban	0.98	-0.003
Rural	0.989	0

2.4 Air temperature

Estimated air temperatures were derived from AVHRR surface temperatures using a simple empirical relation with coefficients determined from the comparison of air temperatures observed at meteorological stations with coincident surface temperatures of the AVHRR pixels where these stations were located. Air temperature values at each station that were coincident with the satellite overpass time were collected and results of regression analysis showed that a strong correlation (r=0.84) exist between air temperature and surface temperature (*Ts*) at night, and a moderate correlation exists at day(r=0.69) presumably reflecting stronger sub-pixel variations of surface cover and heat balance regimes. The relations derived were then applied to the AVHRR images in order to convert AVHRR surface temperatures into estimated air temperatures.

$$\text{Day: } T_{air} = 0.3896 \cdot T_s + 15.313$$
$$\text{Night: } T_{air} = 0.8246 \cdot T_s + 6.2324$$

2.5 Precipitable water (PW)

Chrysoulakis et al. (2008) studied the relation between the AVHRR temperature difference $\Delta T = T4 - T5$ (K) and the atmospheric precipitable water *PW* (cm) over Greece using daytime satellite data and radiosonde data. They found this relation to be essentially linear and approximated by the following equation:

$$PW=0.719 \cdot \Delta T+0.362$$

For nighttime images a relation from Choudhury et al. (1995) was found more suitable, and for urban surfaces is expressed as:

$$PW=1.265 \cdot \Delta T+ 1.493$$

It should be mentioned that **Sta**thopoulou et al. (2005) used a relation from Smith (1966) which gives precipitable water PW (cm) as a function of dew point temperature Td(°F). For the period of summer and the latitudinal zone of Greece Td in °C is obtained from the following equation:

$$T_d = \frac{5}{9}\left(\frac{lnPW + 1.2527}{0.0393} - 32\right)$$

2.4 Relative humidity (*RH*)

Relative humidity (*RH* %) is defined as the ratio of vapor pressure (*e*) to saturated vapor pressure (es) at the air temperature (Ta) expressed as a percent:

$$RH = 100\ \left[\frac{e}{e_s T_a}\right]$$

In this study, vapor pressure and saturated vapor pressure values (in *kPa*) were computed by using the Tetens formulae expressed as:

$$e_s T_a = 0.61078\ e^{\frac{17.269Ta}{Ta+237.29}}$$
$$e\ = e_s T_d$$

2.5 Discomfort index (*DI*)

Thom’s discomfort index (DI) is expressed by a simple linear equation based on dry-bulb (*Tdry*) and wet-bulb (*Twet*) temperatures. Its original form is given as:

$$DI(°F)=0.4(Tdry+Twet)+15$$

If air temperature (*Ta*) as measured in degrees Celsius and relative humidity (*RH)* in % are given, DI can be computed by using the following equation:

$$DI(°C)= Ta – 0.55(1 - 0.01RH)(Ta -14.5)$$

The classes of DI are presented in Table 2 where it can be seen that the human discomfort increases as the Di values increases.

Table 2. Classes of discomfort index

Class number	Di(°C)	Discomfort conditions
1	DI<21	No discomfort
2	21≤DI<24	Less than 50% feels discomfort

3	24≤Di<27	More than 50% feels discomfort
4	27≤DI<29	Most of the population feels discomfort
5	29≤DI<32	Everyone feels severe stress
6	DI≥32	State of medical emergency

3. RESUTS AND CONCLUSIONS

Table 3 shows the mean land surface temperatures by land cover type for daytime and nighttime in the greater Athens area during heat waves. Surface urban heat island is evident at night as urban areas are 4.5°C warmer than rural areas and 2.3°C warmer than suburban areas. This is illustrated in Figure 1 where dark to bright tones indicate cooler to warmer surface temperature. At daytime urban areas are warmer than suburban areas as expected by 2°C but rural areas seem to warmer than urban areas. This can be attributed to the surface characteristics of Athens rural areas as the vegetation percentage is too low and the surface can be described as bare ground. In addition heat waves usually occur in July and August after many weeks of very low or no precipitation and the ground is deficient in moisture. Figure 2 illustrates the mean surface temperature values during heat waves at daytime.

Table 3.Mean values of Ts by land cover type

Land cover type	Daytime Ts(°C)	Nighttime Ts(°C)
Urban	51.5	29.8
Suburban	49.5	27.5
Rural	52.6	25.2

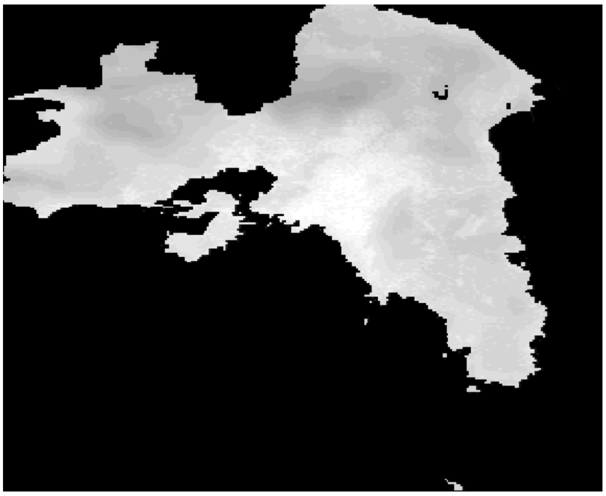

Figure1: Mean land surface temperature map at nightime.

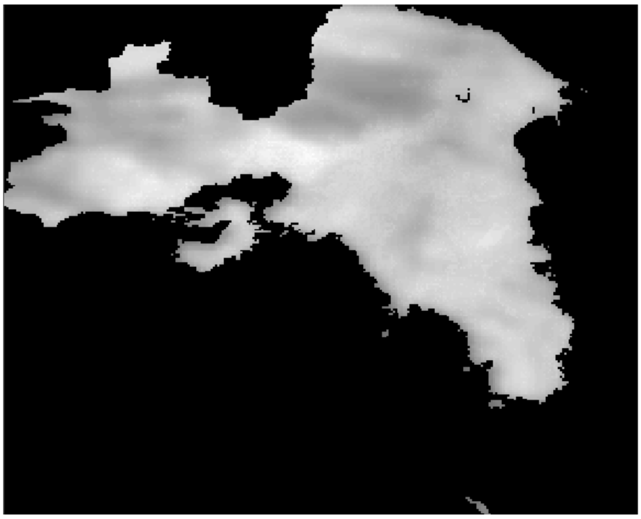

Figure 2: Mean land surface temperature at daytime.

Mean Discomfort Index values during heat waves appear in Table 4. At daytime the suburban areas of Athens have smaller DI values than urban and rural areas. Suburban areas are categorized as “Over 50% of the population feels discomfort” in the DI classification system (Table 2). Urban and rural areas are categorized as “Most of the population suffers discomfort”. Figure 3 illustrates the mean DI values during heat waves at daytime where dark to bright tones indicate lower to higher DI values. At nighttime when the SUHI is relative strong, urban areas have larger DI values than suburban and rural areas. Urban and suburban are categorized as “Over 50% of the population feels discomfort” in the DI classification system. Rural areas are categorized as “Less than 50% of the population feels discomfort”. This is illustrated in Figure 4.

Table 4.Mean values of DI by land cover type

Land cover type	Daytime DI(°C)	Nighttime DI(°C)
Urban	28.1	25.5
Suburban	26.7	24.3
Rural	28.1	22.7

Figure 3. Mean DI values at daytime.

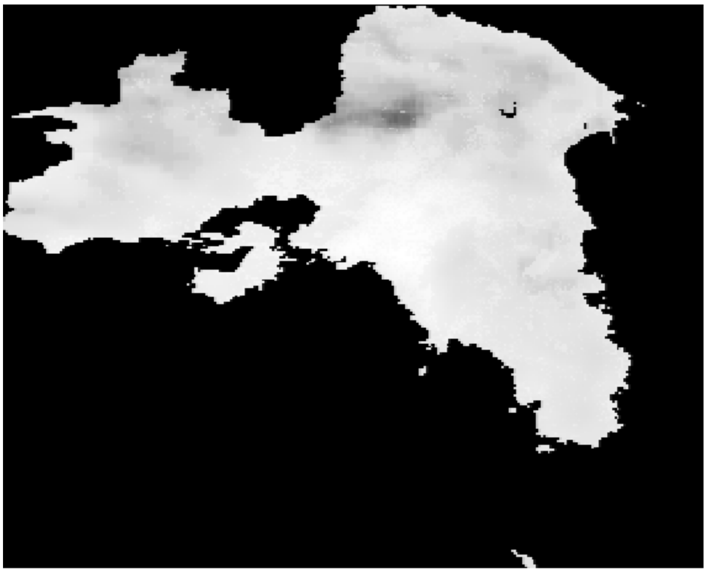

Figure 4. Mean DI values at nighttime.

In this study an attempt was made to verify the presence of surface heat island, to estimate its strength as well as to evaluate Thom’s discomfort index DI in the greater Athens area in the event of summer heat waves. Results demonstrate the capacity of the methodology to assess the state of thermal environment in urban agglomerations and to provide valuable information in support of the protection of the citizens during heat waves.

REFERENCES

A. Bitan The high climatic quality of city of the future Atmos. Environ., 26B (1992), pp. 313–329

Caselles, V., Coll, C., and Valor, E., 1997, Land surface emissivity and temperature determination in the whole HAPEX–Sahel area from AVHRR data. International Journal of Remote Sensing, 18, 1009–1027.

Choudhury, B.J., T.J. Dorman, and A.Y. Hsu, "Modeled and observed relations between the AVHRR split window temperature difference and atmospheric precipitable water over land surfaces", Remote Sensing of Environment, 51 p. 281-290, 1995.

Chrysoulakis, N. and C. Cartalis, "Improving the estimation of land surface temperature for the region of Greece: adjustment of a split window algorithm to account for the distribution of precipitable water". International Journal of Remote Sensing, 23(5): p. 871-880, 2002.

Chrysoulakis, N., Y. Kamarianakis, L. Xu, Z. Mitraka, and J. Ding (2008), Combined use of MODIS, AVHRR and radiosonde data for the estimation of spatiotemporal distribution of precipitable water,J. Geophys. Res., 113, D05101

Coll, C., Caselles, V., Sobrino, J. A., and Valor, E., 1994, On the atmospheric dependence of the split window equation for land surface temperature. International Journal of Remote Sensing, 15, 105–122.

G. Mihalakakou, M. Santamouris, N. Papanikolaou, C. Kartalis, A. Tsagrassoulis. Simulation of the urban heat island intensity in Mediterranean climates by neural networks—a study of the influence of climatic parameters on heat island intensity J Pure Appl Geophys, 161 (2004), pp. 429–451

M. Stathopoulou, C. Cartalis, I. Keramitsoglou, M. Santamouris. Thermal remote sensing of Thom's Discomfort Index (DI): Comparison with in situ measurements Proceedings of the Remote Sensing 2005 Symposium, (SPIE 2005), Brugge, Belgium, 19 September 2005, Environmental Monitoring, GIS Applications, and Geology V, Vol. 5983 (2005), p. 59830K

M. Stathopoulou, C. Cartalis, I. Keramitsoglou Mapping micro-urban heat islands using NOAA/AVHRR images and CORINE land cover: an application to coastal cities of Greece International Journal of Remote Sensing, 25 (12) (2004), pp. 2301–2316

Oke T.(1987) City size and urban heat island, perspectives on wilderness: Testing the theory of restorative environments, proceedings of the Fourth World Wilderness Congress, 7: 769-779

Roth, M., T.R. Oke and W.J. Emery, 1989. Satellite- Derived Urban Heat Islands from 3 Coastal Cities and the Utilization of Such Data in Urban Climatology. International Journal of Remote Sensing, 10 (11): pp. 1699-1720.

Santamouris, M., et al., 2001. On the impact of urban climate on the energy consumption of buildings. Solar Energy, 70 (3): pp. 201-216.

Saunders, R. W., and Kriebel, K. T., 1988, An improved method for detecting clear sky and cloudy radiances from AVHRR data. International Journal of Remote Sensing, 9, 123–150.

Stathopoulou M.,Cartalis C., Andritsos A., 2005. Assessing the thermal environment of major cities in Greece. In: Proc. 1st International Conference on Passive and Low Energy Cooling for the Built Environment, Santorini, Greece.

Thom, E.C., "The discomfort index", Weatherwise, 12: p.57-60, 1959.

Voogt, J.A. and T.R. Oke, 2003. Thermal remote sensing of urban climates. Remote Sensing of Environment, 86 (3): pp. 370-384.